CORA Cork Open Research Archive
Cartlann Taighde Oscailte Chorcaí

| | |
|---|---|
| Title | Generation of 21.3 Gbaud 8PSK signal using an SOA-based all-optical phase modulator |
| Authors | Dailey, James M.;Webb, Rod P.;Manning, Robert J. |
| Publication date | 2011-12-12 |
| Original Citation | Dailey, J. M.; Webb, R. P.; Manning, R. J. (2011) 'Generation of 21.3 Gbaud 8PSK signal using an SOA-based all-optical phase modulator'. Optics Express, 19 (26):B12-B17. doi: http://dx.doi.org/10.1364/OE.19.000B12 |
| Type of publication | Article (peer-reviewed) |
| Link to publisher's version | http://www.opticsinfobase.org/oe/abstract.cfm?URI=oe-19-26-B12 - 10.1364/OE.19.000B12 |
| Rights | © 2011 Optical Society of America. Open Access. - https://creativecommons.org/licenses/by/4.0/ |
| Download date | 2026-11-06 07:58:17 |
| Item downloaded from | https://hdl.handle.net/10468/483 |

UCC
University College Cork, Ireland
Coláiste na hOllscoile Corcaigh

# Generation of 21.3 Gbaud 8PSK signal using an SOA-based all-optical phase modulator

**J. M. Dailey,* R. P. Webb, and R. J. Manning**

*Tyndall National Institute & Department of Physics, University College Cork, Lee Maltings, Cork, Ireland*
**james.dailey@tyndall.ie*

**Abstract:** We describe a novel SOA-based all-optical pure-phase modulator, and show how deleterious cross-gain modulation from the SOAs can be suppressed by utilizing an integrated interferometer structure. We experimentally demonstrate the use of the optical gate as a π/4 phase modulator producing 21.3 Gbaud 8PSK from 21.3 Gbit/s OOK and 21.3 Gbaud QPSK inputs. The modulator produces 3 dB of gain and coherent detection-based bit error rate measurements indicate a 2.4 dB excess penalty.

© 2011 Optical Society of America

**OCIS codes:** (060.0060) Fiber Optics and Optical Communications; (250.4110) Modulators; (250.5980) Semiconductor Optical Amplifiers; (230.1150) All-optical devices; (060.5060) Phase Modulation; (230.0250) Optoelectronics.

## References and links

1. C. Kim and G. Li, "Direct-detection optical differential 8-level phase-shift keying (OD8PSK) for spectrally efficient transmission," Opt. Express **12**(15), 3415–3421 (2004).
2. C. Schmidt-Langhorst, R. Ludwig, D.-D. Gross, L. Molle, M. Seimetz, R. Freund, and C. Schubert, "Generation and Coherent Time-Division Demultiplexing of up to 5.1 Tb/s Single-Channel 8-PSK and 16-QAM Signals," in *Optical Fiber Communications Conference*, OSA Technical Digest (CD) 2009, Paper PDPC6.
3. C. Zhang, Y. Mori, K. Igarashi, K. Katoh, and K. Kikuchi, "Ultrafast Operation of Digital Coherent Receivers Using Their Time-Division Demultiplexing Function," J. Lightwave Technol. **27**(3), 224–232 (2009).
4. X. Zhou, J. Yu, D. Qian, T. Wang, G. Zhang, and P. D. Magill, "High-Spectral-Efficiency 114-Gb/s Transmission Using PolMux-RZ-8PSK Modulation Format and Single-Ended Digital Coherent Detection Technique," J. Lightwave Technol. **27**(3), 146–152 (2009).
5. X. Zhou and J. Yu, "Multi-Level, Multi-Dimensional Coding for High-Speed and High-Spectral-Efficiency Optical Transmission," J. Lightwave Technol. **27**(16), 3641–3653 (2009).
6. N. Kikuchi and S. Sasaki, "Improvement of chromatic dispersion and differential group delay tolerance of incoherent multilevel signaling with receiver-side digital signal processing," in *Optical Fiber Communication Conference*, OSA Technical Digest (CD) 2010, Paper OWV6.
7. M. Nakamura, Y. Kamio, and T. Miyazaki, "M-PSK Versatile Modulation Using a Single-Electrode Straight-Line Phase Modulator and Digital Signal Processing for ISI-Suppression," in *Optical Fiber Communication Conference*, OSA Technical Digest (CD) 2010, Paper OMK8.
8. S. Tsukamoto, K. Katoh, and K. Kikuchi, "Coherent demodulation of optical 8-phase shift-keying signals using homodyne detection and digital signal processing," in *Optical Fiber Communication Conference*, OSA Technical Digest (CD) 2006, Paper OThR5.
9. E. Tipsuwannakul, M. Skold, M. Karlsson, and P. Andrekson, "Transmission of 240 Gb/s PM-RZ-D8PSK over 320 km in 10 Gb/s NRZ-OOK WDM System," in *Optical Fiber Communication Conference*, OSA Technical Digest (CD) 2010, Paper OMJ2.
10. T. Sakamoto, A. Chiba, and T. Kawanishi, "Electro-Optic Synthesis of 8PSK by Quad-Parallel Mach-Zehnder Modulator," in *Optical Fiber Communication Conference*, OSA Technical Digest (CD) 2009, Paper OTuG4.
11. K. Mishina, S. Kitagawa, and A. Maruta, "All-optical modulation format conversion from on-off-keying to multiple-level phase-shift-keying based on nonlinearity in optical fiber," Opt. Express **15**(13), 8444–8453 (2007).
12. K. Mishina, S. M. Nissanka, A. Maruta, S. Mitani, K. Ishida, K. Shimizu, T. Hatta, and K. Kitayama, "All-optical modulation format conversion from NRZ-OOK to RZ-QPSK using parallel SOA-MZI OOK/BPSK converters," Opt. Express **15**(12), 7774–7785 (2007).
13. I. Kang, M. Rasras, L. Buhl, M. Dinu, S. Cabot, M. Cappuzzo, L. T. Gomez, Y. F. Chen, S. S. Patel, N. Dutta, A. Piccirilli, J. Jaques, and C. R. Giles, "Generation of 173-Gbits/s single-polarization QPSK signals by all-optical format conversion using a photonic integrated device," in *35th European Conference on Optical Communication,* (2009), Paper 10.3.1.
14. I. P. Kaminow, T. Li, and A. E. Willner, *Optical Fiber Telecommunications V A: Components and Subsystems* (Academic Press, 2008). Ch. 7.

#154148 - $15.00 USD Received 6 Sep 2011; revised 1 Nov 2011; accepted 1 Nov 2011; published 16 Nov 2011
(C) 2011 OSA

15. I. Kang, M. S. Rasras, L. Buhl, M. Dinu, G. Raybon, S. Cabot, M. A. Cappuzzo, L. Gomez, Y. Chen, S. S. Patel, A. Piccirilli, J. Jaques, and C. R. Giles, "High-Speed All-Optical Generation of Advanced Modulation Formats Using Photonic-Integrated All-Optical Format Converter," IEEE Journal of Selected Topics in Quantum Electronics, *Published Online, http://ieeexplore.ieee.org/xpls/abs_all.jsp?arnumber=5771528*.
16. J. M. Dailey and T. L. Koch, "Simple Rules for Optimizing Asymmetries in SOA-Based Mach-Zehnder Wavelength Converters," J. Lightwave Technol. **27**(11), 1480–1488 (2009).
17. T. Durhuus, B. Mikkelsen, C. Joergensen, S. Lykke Danielsen, and K. E. Stubkjaer, "All-optical wavelength conversion by semiconductor optical amplifiers," J. Lightwave Technol. **14**(6), 942–954 (1996).
18. W. Jin, A. Maitra, C. G. Poulton, W. Freude, and J. Leuthold, "Temporal Dynamics of the Alpha Factor in Semiconductor Optical Amplifiers," J. Lightwave Technol. **25**(3), 891–900 (2007).
19. R. J. Essiambre, G. Kramer, P. J. Winzer, G. J. Foschini, and B. Goebel, "Capacity Limits of Optical Fiber Networks," J. Lightwave Technol. **28**(4), 662–701 (2010).

## 1. Introduction

Demands for higher capacity in deployed fiber optic networks have spurred research into high-level advanced modulation formats with increased spectral efficiency. One promising modulation format is 8-phase-shift keying (8PSK) where the modulation symbols are arranged in a ring constellation providing 3 bits/symbol, which is a 50% increase in spectral efficiency over quaternary(Q)PSK [1–4]. Furthermore, when compared with n-symbol quadrature amplitude modulation (n-QAM) formats, 8PSK's constant symbol amplitude can provide increased robustness against nonlinear fiber transmission impairments [5].

Several techniques for electro-optically generating 8PSK signals have been demonstrated in the literature. A single phase modulator is capable of generating a ring-shaped signal constellation, and high-order PSK formats would generally require multi-level RF drive signals. This has been demonstrated using arbitrary waveform generators driving an IQ modulator [6] as well as a single-electrode straight-line phase modulator [7]. These multi-level schemes may minimize the number of required optical modulators, but the necessary multi-level RF signals can be difficult to generate at high symbol rates. At the expense of multiple optical modulators, schemes employing binary RF driving signals have also been demonstrated including a QPSK modulator followed by a trailing phase modulator [8,9], or a Mach-Zehnder Interferometer (MZI) super-structure incorporating 4 sub-MZIs [10].

However, the generation of high-order PSK formats is not limited to RF-driven electro-optic (EO) devices. Several all-optical techniques for the generation of these advanced modulation formats can also be found in the literature. By all-optical, we refer to the control of a photonic device's transmission properties via optical signals as opposed to electronic signals. For example, DPSK and QPSK signals were generated with on-off keyed (OOK) input signals in [11] using cross-phase modulation in highly nonlinear fiber. Semiconductor optical amplifier (SOA)-based MZI devices fabricated using monolithic [12] and hybrid integration [13] technologies have also been utilized to all-optically produce QPSK.

Much of the previous work in all-optical format generators was motivated by the consideration of modulation format conversions at the interfaces between optical networks. Comparatively little discussion has appeared on the use of these generators as all-optical transmitters and their advantages over EO modulators. Even at moderate symbol rates (< 40 Gbaud) the RF drive amplifiers used with EO modulators can be difficult to design with sufficient bandwidth and output power. The RF data signal delivered to the EO modulator is also degraded by transmission line parasitics resulting in reflections and effective bandwidths much smaller than the intrinsic material electro-optic bandwidth [14]. These impairments could be avoided by using optically-controlled modulators; the control signals can be easily delivered over high-bandwidth waveguides and with sufficient power to control the optical nonlinearity. The latter is especially true in the case where SOAs are used as the nonlinear medium. As Kang, *et al*, have pointed out in [15] the use of optical control signals also allows the aggregation of low-rate tributaries in the optical domain via optical time division multiplexing (OTDM) as opposed to electronic time division multiplexing (ETDM). EO modulators must still be used to provide the control signals for the all-optical modulator, but the use of OTDM may ameliorate the RF design issues discussed above. The combination of electronic and optical control signals increases the flexibility in optimizing optical

#154148 - $15.00 USD Received 6 Sep 2011; revised 1 Nov 2011; accepted 1 Nov 2011; published 16 Nov 2011
(C) 2011 OSA

transmitters at low symbol rates, and also provides a clear path to symbol generation rates well beyond the current reach of electronics (>> 40 Gbaud).

In this paper, we report for the first time on the use of a novel all-optical π/4 phase modulator for the generation of an 8PSK output signal from QPSK and OOK input signals. The optically-controlled phase modulator consists of an integrated SOA-based MZI structure [16, 17]. We demonstrate 21.3Gbaud 8PSK generation using the proposed method and measure 3dB of signal gain at the gate output. Coherent detection was employed to evaluate the performance, and we measure a 2.4dB excess bit error rate (BER) penalty.

## 2. Theory of operation

When an intense optical pump pulse is injected into an SOA, the resultant change in carrier density modifies the gain and refractive index seen by any co-propagating probe signals at other wavelengths. These are the well-known nonlinear cross-gain and cross-phase modulation (XGM and XPM) phenomena [16], and the gain and phase changes are often related to each other through the α-factor [18]:

$$\alpha = \frac{-4\pi}{\lambda}\frac{\delta n}{\delta g} = -2\frac{\delta\varphi}{1n\{G_f / G_i\}} \tag{1}$$

where λ is the probe wavelength while δn and δg are the changes in refractive index and material gain resulting from the pump pulse, respectively. δφ represents the probe phase change, while $G_f$ and $G_i$ are the final (saturated) gain and initial (unsaturated) gain, respectively.

An ideal optically controlled phase modulator will produce output symbols of constant amplitude. This suggests a requirement that for single-SOA phase modulators there must be zero XGM, i.e. an infinite α-factor. This is an unrealistic requirement in practice, and so the XGM must somehow be suppressed in SOAs with finite α-factors. This can be accomplished by embedding a pair of SOAs in a Mach-Zehnder interferometer (MZI) structure. The extra degree of freedom provided by the MZI bias point enables the cancellation of XGM. The basic optical gate configuration is shown below in Fig. 1.

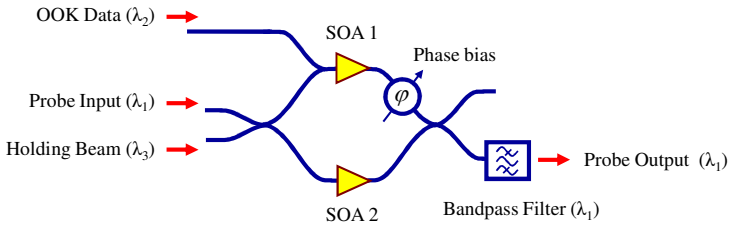



Fig. 1. SOA-based MZI all-optical phase modulator. Control of the phase bias allows effective suppression of the deleterious XGM.

An input probe symbol is split at the first MZI coupler, propagates through SOA1 and SOA2, and then recombines at the output coupler. The MZI phase bias control varies over 2π radians and controls the interference conditions at the output coupler. The binary effect of the optical gate on an input symbol can be modeled using two transfer functions: $H_0$ and $H_1$ for OOK input symbols of 0 (no pulse) and 1 (pulse), respectively. These functions are given below in Eqs. (2)-(3) for an unsaturated SOA gain normalized to unity:

$$H_0 = \frac{1}{2}[1 + e^{j\varphi}] \tag{2}$$

$$H_1 = \frac{1}{2}[1 + e^{-\delta\varphi/\alpha}e^{j(\varphi+\delta\varphi)}] \tag{3}$$

#154148 - $15.00 USD Received 6 Sep 2011; revised 1 Nov 2011; accepted 1 Nov 2011; published 16 Nov 2011
(C) 2011 OSA

where φ is the phase bias control shown in Fig. 1 and δφ is the XPM induced on the input symbol in SOA1. The XGM is expressed in terms δφ by invoking the α-factor on the right hand side of Eq. (3).

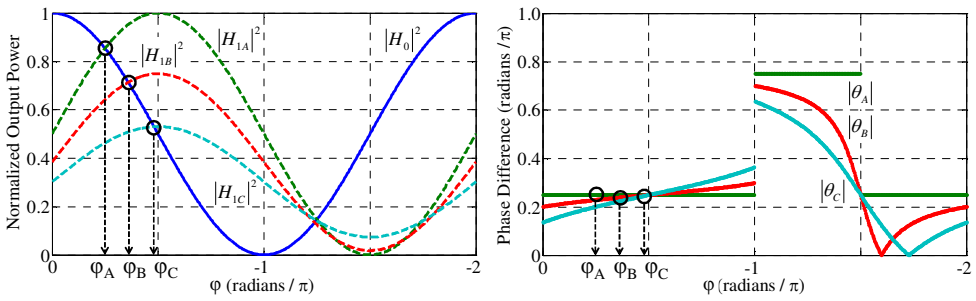



Fig. 2. (a) The normalized output powers from the MZI as a function of static phase shift, φ. $H_0$ (solid line) is calculated from Eq. (2). $H_{1A}$, $H_{1B}$, and $H_{1C}$ (dashed lines) are calculated from Eq. (3) using $\alpha = 10^6$ (i.e. ∞), 5, and 2, respectively. The XPM shift (δφ), is $0.5\cdot\pi$ in all three cases. (b) The relative phase angle between $H_1$ and $H_0$ as a function of static phase, φ. The three plots correspond with the three α-factor values in (a).

The normalized MZI output powers (i.e. magnitude of H squared) are plotted in Fig. 2(a) as a function of the static phase shift, φ. The solid line corresponds to the unpumped modulator (H0). The three dashed lines are plots of H1 for a XPM shift (δφ) of 0.5π radians using three different representative α-factor values. H1A, H1B, and H1C are calculated using α = 106 (~∞), 5, and 2, respectively. H1A depicts the output when there is no XGM. The power response in this case is simply translated to the right by 0.5π radians. H1B and H1C show the effect of increasingly large XGM shifts on the output power of the MZI.

The key operating principle of this phase modulator is that φ can be chosen at a crossing point of $H_0$ and $H_1$ in order to equalize the two output powers, even in the presence of XGM. $H_0$ and $H_1$ exhibit two crossing points within 2π radians of φ, and one of these power-equalization points will generally provide a higher output power than the other. These three high-power points are labeled in Fig. 2(a) as φ = $\varphi_A$, $\varphi_B$, and $\varphi_C$. For example, $|H_0(\varphi=\varphi_A)|^2 = |H_{1A}(\varphi=\varphi_A)|^2$. Even though the amplitudes of the two possible output symbols can be equalized in this way, the XGM effectively reduces the output power available from the phase modulator.

The angle between the two output symbols, i.e. the phase modulation, from the optical gate is also a function of φ. This angle is denoted by θ and is calculated using Eqs. (2)-(3):

$$\theta_A = \angle H_{1A} - \angle H_0 \tag{4}$$

where $\theta_B$ and $\theta_C$ are defined similarly. The magnitudes of these angles are plotted in Fig. 2(b) for static phase φ varying over 2π radians. The discontinuities in θ coincide with the phase inversions of $H_0$ and $H_1$ with the changing static phase, φ. The phase modulation is calculated at the point where the output symbols are equal in amplitude, e.g. $\theta_A(\varphi = \varphi_A)$. In Fig. 2(b), the increasing amount of XGM slightly alters the available phase modulation in the region between $\varphi_A$ and $\varphi_C$. In this example, regardless of the α-factor, for a XPM shift of 0.5π the output phase modulation is ~0.25π. In general, the desired output symbol modulation can be achieved by changing the magnitude of the XPM through adjustment of the input OOK pump power.

The results summarized in Fig. 2 suggest that φ can be used to adjust the ratio of output symbol amplitude modulation to phase modulation. We can define an effective α-factor for the phase modulator as follows:

$$\alpha_{eff} = -2\frac{\theta}{1n\{|H_1|^2 / |H_0|^2\}} \tag{5}$$

#154148 - $15.00 USD Received 6 Sep 2011; revised 1 Nov 2011; accepted 1 Nov 2011; published 16 Nov 2011
(C) 2011 OSA

which is similar in form to Eq. (1). The preceding discussion focused on driving Eq. (5) to infinity by forcing the denominator to zero. This enables the MZI gate to operate as an ideal pure-phase modulator. Having control over $\alpha_{eff}$ may also allow other advanced modulation formats to be realized with this phase modulator, for example 2ASK/4PSK.

## 3. Experimental results

The experimental setup used to evaluate the SOA-based π/4 phase modulator is shown below in Fig. 3. An ERGO mode-locked laser (MLL) operating at 10.65 GHz generated ~2.1 ps optical pulses at $\lambda_1$ = 1562 nm which were modulated using a standard $2^7$-1 PRBS to produce a 10.65 Gbaud binary phase-shift-keyed (BPSK) signal. This optical signal was then passively multiplexed up to 21.3 Gbaud BPSK and passed through a delayed interferometer (DI) to produce a 21.3 Gbaud QPSK signal. The DI had a free spectral range of 10.65 GHz and the relative phase shift between the two interferometer arms was set to +/− π/2. This QPSK signal was injected into the optical gate as the probe signal (see Fig. 1). We note that a rigorous systems test should incorporate a QPSK modulator driven by decorrelated I/Q data streams, but this QPSK signal is sufficient for a proof-of-concept demonstration.

Another MLL ($u^2t$) generated ~2.6 ps optical pulses at $\lambda_2$ = 1550 nm and with the same 10.65 GHz clock rate. The pulses were OOK-modulated with an inverted $2^7$-1 PRBS, multiplexed up to 21.3 Gb/s, and injected into the optical gate as the pump (see Fig. 1). The pump and probe data sequences were appropriately decorrelated from each other temporally. A continuous wave (cw) holding beam at $\lambda_3$ = 1555 nm was also injected into the interferometer input to saturate the SOAs and reduce their recovery times.

The optical gate is a hybrid-integrated device manufactured by CIP Technologies. The proprietary buried-heterostructure SOAs were fabricated using III-V materials and then hybrid-integrated with low-loss planar silica waveguides. The SOAs were both biased ~355 mA with amplified spontaneous emission (ASE) peaks at ~1560 nm. The QPSK, OOK, and holding beam input powers were −5 dBm, + 2 dBm, and −2 dBm, respectively. The 8PSK output power from the optical gate was −2 dBm, indicating a signal gain of 3 dB.

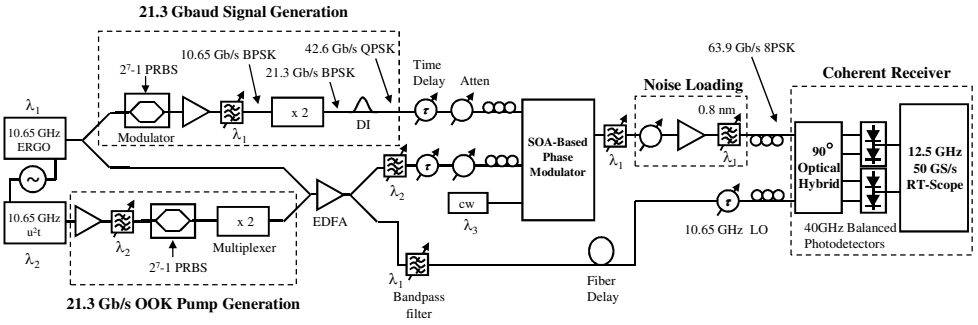



Fig. 3. Experimental setup used to test the all-optical phase modulator.

Prior to coherent detection, the 8PSK signal was injected into an EDFA for noise loading. The local oscillator (LO) signal was provided by the 10.65 GHz clock output from the ERGO. A fiber delay matched the overall signal and LO path lengths in order to minimize the impact of the ERGO's linewidth on receiver performance. The 90° hybrid output signals were converted to photocurrent using balanced photodetectors and sampled by a real-time scope at 50 GS/s for offline processing in Matlab. The in-phase and quadrature-phase traces were upsampled to an integer number of samples per symbol. The complex signal was then reconstructed using one sample per symbol which was followed by phase estimation and symbol discrimination. Errors were counted in the demodulated data, and the BER was calculated assuming the PSK signals have been Gray mapped. The LO operated at half the PSK symbol rate and as a result each time-division multiplexed (TDM) sub-channel was captured individually and analyzed for BER.

#154148 - $15.00 USD Received 6 Sep 2011; revised 1 Nov 2011; accepted 1 Nov 2011; published 16 Nov 2011
(C) 2011 OSA

BERs are shown below in Fig. 4(a). 106.5k symbols were acquired for each data point in Fig. 4(a). The QPSK Input traces are the two TDM channels measured before injection into the optical gate. The QPSK Output traces are the two unmodulated TDM channels measured after the gate with the OOK pump signal turned off. The mean penalty at a BER = $10^{-3}$ is 1.4 dB. We believe this penalty arises in part due to ASE from the SOAs and some possible signal distortion. The 8PSK Output traces are the modulated outputs from the gate. The mean penalty with respect to the unmodulated QPSK output signals is 7.7 dB, and thus the total modulation penalty is 9.1dB. Comparing the 7.7 dB penalty with the theoretical penalty of 5.3 dB for converting QPSK to 8PSK [19] we calculate an excess penalty of only 2.4dB. This penalty is comparable to work by Tsukamoto, *et al*, on generation of 10 Gbaud 8PSK [8].

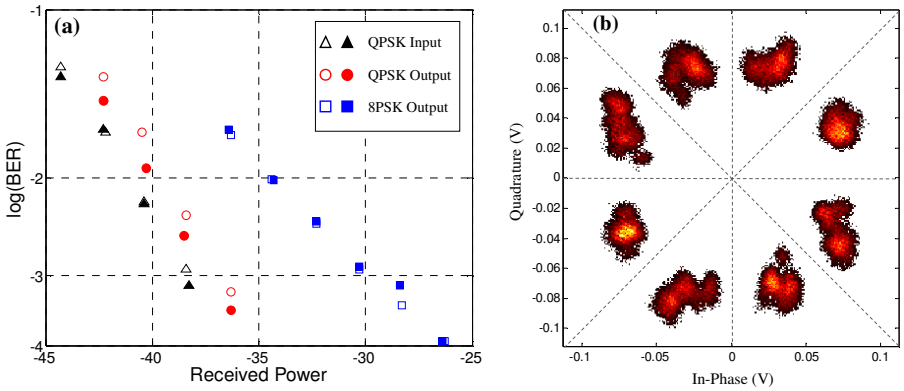



Fig. 4. (a) BER curves for the two input QPSK TDM tributaries (triangles), the two QPSK tributaries after the all-optical modulator when the OOK pump is turned off (circles), and the two 8PSK output tributaries (squares). The received power is the total power for both tributaries and is measured at the input to the "Noise Loading" EDFA shown in Fig. 3. (b) Histogram generated from a measured 8PSK signal constellation.

## 4. Conclusions

We have proposed and experimentally verified a novel all-optical phase modulator operating at 21.3 Gbaud. We have shown how the proper choice of MZI phase bias can suppress SOA XGM while using the XPM for generating pure-phase modulated output symbols. BER measurements show a 1.4dB penalty for unmodulated QPSK output signals from the all-optical modulator, and only a 2.4dB further excess penalty for format conversion to 8PSK.

Other modulation formats should also be achievable using this optical gate. For example, by tuning the phase bias a 2ASK/4PSK [19] output modulation should be possible. This transmitter scheme relies on fast optical nonlinearities, and provides a potential path to ultrafast symbol generation beyond the current reach of electro-optic modulators [13].


## Acknowledgments

The authors wish to thank Prof. Andrew Ellis and Selwan Ibrahim for several helpful discussions, as well as Paul Townsend's group for lending the real-time scope. This work was funded under Science Foundation Ireland grant 06/IN/1969.


#154148 - $15.00 USD Received 6 Sep 2011; revised 1 Nov 2011; accepted 1 Nov 2011; published 16 Nov 2011
(C) 2011 OSA